

THE CASE FOR FLUX PUMPS AND SOME OF THEIR PROBLEMS

S.L. Wipf
Atomics International
A Division of North American Rockwell Corporation
Canoga Park, California

I. INTRODUCTION

As an introduction to this morning's session let me recapitulate the principle of flux pumping.

Complete lack of resistance in a closed circuit leads to conservation of magnetic flux linked with it. We see this by writing Faraday's induction law for a closed circuit with inductance L_c :

$$\frac{d\Phi}{dt} = -V = -RI - d(L_c I)/dt \quad (1)$$

With resistance $R = 0$, this integrates to:

$$\Phi + L_c I = \text{const.} \quad (2)$$

The superconducting circuit meets any change in external flux Φ with a corresponding change in current to fulfill Eq. (2). A flux pump is a device which can change the constant in Eq. (2). Figure 1 shows the flux pump principle. Flux from a small permanent magnet does not enter a superconducting circuit (Fig. 1a) until a switch is opened and closed again (Fig. 1b). On removal of the magnet the current ΔI will then preserve the flux (Fig. 1c). To accumulate more current by repetition of this process, care is taken that the previously induced current is not lost during switching. One provides a bypass which itself has a switch (Fig. 1d). To make a pump practical one has to avoid mechanical switches (although for small currents they are feasible and have certain advantages¹). It is sufficient, instead, to introduce some resistance by locally destroying superconductivity. This can be done by exceeding the critical temperature of the superconductor, using a heater as in some of the earliest pumps,^{2,3} or else by exceeding the critical field. This last approach, magnetic switching, is the most widely used. In its simplest version the same magnet which is used for pumping (the exciting or energizing magnet) is also used for switching because close to the poles the field strength easily exceeds the critical field of superconductors such as lead or niobium (with critical fields of 550 G or ~ 3000 G at 4.2°K). The magnetic switching method also allows the replacement of the loop in Fig. 1d by a plate in Fig. 1e. The high field right in front of the magnet pole will form a normal zone containing the flux and by moving this zone across the sheet - it follows the magnet -

-
1. I.D. McFarlane, *Cryogenics* 7, 297 (1967); see also: *Product Engineering*, Feb. 27, 1968, p. 27.
 2. A.F. Hildebrandt, D.D. Elleman, F.C. Whitmore, and R. Simpkins, *J. Appl. Phys.* 33 2376 (1962); D.D. Elleman and A.F. Hildebrandt, in *Proc. 8th Intern. Conf. Low Temperature Physics*, London, 1962 (Butterworth, London, 1963), p. 332.
 3. H.L. Laquer, *Cryogenics* 3, 27 (1963).

the same function as in Fig. 1d is performed.⁴ The arrangement is, of course, such that the removal of the magnet from the circuit occurs without interrupting the superconductivity; the circuit (other than the loop or the plate) may be located far away from the pole so that the critical field of the circuit superconductor is nowhere reached and usually it is made out of high field material anyway.

Flux pumps can be operated mechanically (Fig. 1e) or without moving parts as in Fig. 2 where a "loop" and a "plate" arrangement is shown. It is practical to distinguish between "moving magnetic field" type pumps of which this plate pump is an example, as well as that of Fig. 1, and "rectifier" type pumps, illustrated by the upper example of Fig. 2. The next paper (Rhodenizer) will detail the rectifier pump which has been developed by GE⁵ to a high perfection. The present paper will emphasize the moving magnetic field type.

II. THE CASE FOR FLUX PUMPS

Once the idea is presented it seems to be obvious that one should use flux pumps as soon as a current source, or power, is needed in liquid helium. The only viable alternative is current leads from room temperature into the cryogenic environment. Lubell will compare the two.

One might think that the dc transformer suggested by Giaever⁶ could provide another alternative. This device is akin to the flux pump illustrated in Fig. 1e. We imagine the plate seen there, which is the secondary, to be very thin and to be sandwiched together with another very thin plate or film, which is the primary, with an insulating oxide layer in between. All thicknesses have to be small compared to the spacing of fluxoids which will thread both films at right angle and which may be produced by a stationary field which is smaller than the critical field. The fluxoids are set into motion by the Lorentz force of a current (parallel to the secondary current to be induced) passed through the primary film. Due to the closeness of the two films the identical fluxoids which move through the primary are dragged through the secondary and thus perform the same function as the mechanically moved exciting magnets of the flux pump. To date this device has not replaced the flux pump, however, because the fluxoids are "sheared off" and remain stationary in the secondary under the influence of both the pinning forces and the Lorentz force of a rather small secondary current.

Why do we have to plead a case for flux pumps? Why does one who favors them find himself in the role of a salesman or on the defensive? It can hardly be ignorance for there have been good reviews by the groups at Philips⁷ and Leiden.⁸ It may be fear of disadvantages which have perhaps not been spelled out too clearly. If in this morning's session we manage to dispel some of these fears we may be successful in our plea.

-
4. J. Volger and P.S. Admiraal, *Phys. Letters* 2, 257 (1962); also in *Philips Techn. Rev.* 25, 16 (1963).
 5. T.A. Buchhold, *Cryogenics* 4, 212 (1964); T.A. Buchhold, in *Pure and Applied Cryogenics* (Pergamon Press, 1966), Vol. 6, p. 529.
 6. I. Giaever, *Phys. Rev. Letters* 15, 825 (1965), and 16, 460 (1966).
 7. J. Van Suchtelen, J. Volger, and D. Van Houwelingen, *Cryogenics* 5, 256 (1965).
 8. H. Van Beelen, Miss A.J.P.T. Arnold, H.A. Sypkens, J.P. Van Braam Houckgeest, R. De Bruyn Ouboter, J.J.M. Beenakker, and K.W. Taconis, *Physica* 31, 413 (1965).

The following table lists what I consider the advantages and disadvantages of flux pumps (if applicable, the comparison is with conventional power supplies at room temperature and current leads).

<u>Advantages</u>	<u>Disadvantages</u>
Large currents (10^4 - 10^5 A)	Shielding from ambient fields necessary
Persistent mode when idle	
Forward or backward operation	Protection required
Ideally suited to compensate for small resistive losses in circuit	Losses in liquid helium while operating
Over-all space requirement small (same as with superconducting magnets)	Volume inside cryostat required ($\sim 50 \text{ cm}^3/\text{W}$) therefore small power
Flexible (can operate at several times rated optimum output power at the price of increased losses)	

III. SOME PROBLEMS

The remainder of this talk will be devoted to the problems as they are encountered in moving magnetic field pumps if one strives to develop a theory or to increase either the efficiency or the ultimate current.

Theory

One of the simplest examples of a pump which is in practical use is illustrated in Fig. 3. Its main feature is a normal zone which is moved through a superconducting sheet without ever entering or leaving it. Mathematical treatments of similar arrangements⁹⁻¹¹ do exist and have been tested experimentally^{9,10,12} with what one could term semiquantitative success. They produce formulae for the output voltage and for the loss,

$$\text{emf} = n \cdot \omega (P - L_p I_{\text{load}}) \quad (3)$$

$$\text{Loss} = n \cdot \omega L_p I(0)^2 \quad (4)$$

The rotation speed, ω , is assumed to be small enough to neglect terms with ω^2 . n is the number of poles of the rotor, I the load current, and P the flux per normal spot due to the rotor poles. L_p is an effective inductance, and $I(0)$ an effective current. In practice these effective quantities are adjustable parameters which cannot be calculated. This considerably spoils the success of the mathematical approach. In fact,

-
9. S.L. Wipf, in Proc. Intern. Symp. Magnet Technology, Stanford, 1965, p. 615.
 10. D. Van Houwelingen and J. Volger, Philips Res. Rep. 23, 249 (1968).
 11. H. Voigt, Z. Naturforsch. 21a, 510 (1966).
 12. R. Weber, Z. Angew. Phys. 22, 449 (1967).

to be quite honest, this lack of a good theory reflects our poor understanding of what seems to be such a simple process as moving a normal spot across a superconducting sheet.

Let us discuss this process in some more detail. Illustrated in Fig. 4 is a normal zone containing flux Φ and moving through a superconducting sheet which carries a load current density. We separate two processes which are indicated by their current patterns. One is the induction of eddy currents within the normal spot. They flow along closed paths, partly within the spot and partly without. Because the size of the eddy currents is proportional to the speed of the spot ($v = 2\pi r\omega$), their over-all contribution to the total voltage and losses of the pump are proportional to v^2 (and higher terms) and have been neglected in the given formulae (3) and (4); eddy currents are reasonably understood and in what follows we shall only consider very low speeds. The other process, which we may call the switching process, takes place in the leading edge of the normal spot (indicated by narrow crosshatching in the figure) where the superconductor is made normal in the presence of a current density j . The ohmic voltage thus generated will drive the current into an alternate distribution while some of it is dissipated. The corrections to the output voltage and the loss are reflected in Eqs. (3) and (4) and will be discussed a little further. Without the switching process the current increase per pump cycle, as seen in Fig. 1, is $\Delta I = \Phi/L_c$. The output voltage, therefore, is given by $L_c dI/dt = L_c \Delta I \omega = \Phi\omega$.

The width Δs of the leading edge depends on the time constant of the switching process and it is therefore inversely proportional to the rotation speed. For simplicity we assume that the normal spot is moved in small steps by a distance equal to the width Δs of the leading edge. Also it is assumed that the initial total current in the leading edge is $I_{e0} = \Delta s \cdot j$, and further that there is current flow only across the narrow ends of the edge (top and bottom in Fig. 4) and that the resistance of the edge is R . Unfortunately, R is not constant and depends on the current as we will discuss later.

The voltage across the leading edge is then, $RI_e = L_e dI_e/dt$, where L_e is the inductance of the alternate current path (which is the short circuit of the edge through the rest of the sheet). We can assume a linear decay of I_e to zero during each step, which gives an average voltage of $L_e I_{e0} 2\pi\omega/\Delta s = L_e j 2\pi\omega$. We can assume that j is not zero when no load current is flowing and that it has a component which is proportional to the load current; thus, $j 2\pi r = I_0 + k I_{load}$. The voltage correction becomes $\omega L_e (I_0 + k I_{load})$ and it is negative (i.e., decreasing I_{load}). Comparison with Eq. (3) gives: $P = \Phi - L_e I_0$, and $L_p = k L_e$.

The loss is obtained similarly. If there are N steps per cycle ($N = 2\pi r/\Delta s$), the loss per cycle becomes $\frac{1}{2} N L_e I_{e0} dI_e/dt = \frac{1}{2} L_e \omega j^2 (2\pi r)^2$. The total loss is $\frac{1}{2} \omega L_e \cdot (I_0 + k I_{load})^2$, and comparison with Eq. (4) gives $L_p = k L_e$, and $I(0) = (I_0 + k I_{load})/\sqrt{2k}$. The factor $1/\sqrt{2k}$ is only a means to keep L_p in both Eqs. (3) and (4) formally unchanged; this is convenient because one usually obtains the quantities P and L_p according to Eq. (3) from measurements of the voltage, and then $I(0)$ from loss measurements.

A word about the various quantities: we now have k , L_e , and I_0 which we can neither measure directly nor calculate. The accuracy of measuring Φ directly is also insufficient to notice the difference between P and Φ . It is useful, however, to have an idea about the formal validity of Eqs. (3) and (4), and we shall see that they can serve as guidelines through the experimental results.

It has already been mentioned that R depends on current. This becomes clear when the leading edge region is described in more detail. At its outer boundary it adjoins the fully superconducting phase with a resistance of zero; at its inner boundary it may be fully normal with the resistivity at the normal constant value. We have, therefore,

to distinguish two parts in this resistive current carrying region which we have called the leading edge: one is fully normal, the resistivity is constant (magnetoresistance and temperature effects are insignificant), and the currents decay exponentially; the other is in the critical state, the external field is below the upper critical value, but the current density is critical making it resistive. This part we call the critical region. The resistivity in the critical region is rather similar to the dynamical resistivity introduced in the discussion of ac losses.* It has to be proportional to dH/dt because of the magnetic diffusion equation; other than that its value is too difficult to calculate.

Critical regions can also be described as regions where magnetic flux moves under the influence of pinning forces. Many problems are easier to visualize by using this concept.

Critical regions are not confined to the leading edge alone, they occur also at the trailing edge of the spot and even in other parts of the pumping sheet. In fact, they do occur wherever the perpendicular field component through the sheet changes with time ($dH_{\perp}/dt \neq 0$) and the total field is less than critical. The leading edge is only different from these other regions in that it also may have a fully normal section which carries current (other than eddy currents).

The situation would be similar if the normal spot were created by exceeding the critical temperature instead of the critical field.¹³ Temperature gradients around the edges would then create the critical regions.¹⁴

Critical regions are always shorted out by alternate current distributions through the fully superconducting parts of the sheet. These distributions, i.e., their inductances, are determined by the flux conservation principle because the sheet with pinning behaves just like a superconducting wire mesh screen trying to conserve the flux through each mesh. To obtain information about critical regions and current distributions one makes field measurements.

In Fig. 5 there is an xy plot of the tangential and radial fields close to the outer surface and at the center of the sheet vs the angular position of the very slowly turning rotor. The sheet consists of a threefold thickness of Nb foil, 0.001 in. thick. This type of pump is illustrated in Fig. 3; the rotor has three wings as illustrated in the insert to Fig. 5. The measured field is a combination of the field due to the rotor, which is given by the zero current line (dashed), and that due to the load current which increases by 450 A per revolution.

A uniform current distribution in the cylindrical sheet would produce zero radial field and a uniform tangential field, somewhat smaller than the increase reflected in the plot (there is a small contribution from the current leads of the circuit). The tangential plot then is not very sensitive to nonuniform distributions, but any contribution to the radial field distribution is entirely due to nonuniformity. The increasing current creates a dip in front of the pole and depresses the front edge while enhancing the back edge of the pole field. An accurate calculation of the current distribution from such field measurements would require still more field profiles near the edges of the sheet, since it is a three-dimensional problem because the rotor is not thick enough to allow a two-dimensional solution. We can guess the current distribution

* See, for example, S.L. Wipf, these Proceedings, p. 511 and p. 683.

13. J.F. Marchand and J. Volger, Phys. Letters 2, 118 (1962).

14. F.A. Otter and P.R. Solomon, Phys. Rev. Letters 16, 681 (1966);

A.T. Fiory and B. Serin, Phys. Rev. Letters 16, 308 (1966).

vs the angle to be roughly triangular between the poles with the maximum current density (the apex of the triangle) closer to the front edge of the pole and shifting towards the middle with increasing current. On the other hand the critical current density, limited by the field of the poles, would have a flat maximum in the middle between the poles and would be otherwise almost symmetrical. It might then be expected that the triangular current distribution could reach the critical current near its apex, but not near the back edge and not even near the front edge of the poles. That this is indeed so can be read from the radial field plot. We see that the radial component undergoes a change between the poles; this indicates a critical region. This region becomes large and moves towards the middle with increasing current.

Another important effect can be observed in Fig. 5. This effect corresponds to a sudden rearrangement of the current distribution as seen at 185° in the curve relating to the radial distribution for 6000 A; the same and similar effects are seen near 210° in the tangential curves (the difference of 25° in position is the distance of the two Hall probes). We call this an instability and it corresponds to a sudden breakdown of the pinning forces which in many other situations is observed and described as flux jump.

Efficiency

A typical setup used to measure the losses is illustrated in Fig. 6. The torque transmitted to the shaft is measured at room temperature. Instead of loops as in Fig. 6, we use a sheet of 0.08 mm thick niobium, in triple thickness. The circuit has four turns of 7.4 cm diameter at the center of which a Hall probe measures the current. A simple potentiometer converts the distortion angle of the torsion spring (approximately $15^\circ/\text{lb in.}$) into a voltage which is calibrated and recorded along with the output current vs the rotation angle. (The device shown in Fig. 6 employs visual torque observation.) Such a record is shown in Fig. 7.

We recognize two new features. One is the relaxation angle between zero and full torque, the other the irregular small jumps as the rotation proceeds under full torque while the current increases steadily. These can easily be interpreted as consequences of flux pinning as is illustrated in the accompanying qualitative picture, which shows a pole at rest, and a pole before reaching full torque. Flux pinning occurs between a lower critical field (H_{c1}) and an upper critical field (H_{c2}), this region being shaded in the picture. It can be seen how the distortion of the flux lines increases the extent of this region, before the flux pattern, which will move with the pole, reaches an equilibrium. Even this equilibrium movement will occur in small jumps due to instabilities caused by the inhomogeneities in the flux pinning strength. The shaded regions adjacent to the moving spot can be identified with the critical regions discussed above.

In Fig. 8 are shown input equilibrium torques measured and plotted in this manner vs P, in units of joules/rotation ($1 \text{ J/rot} = 1.59 \times 10^6 \text{ dyn}\cdot\text{cm} = 1.41 \text{ lb}\cdot\text{in.}$). Also given is the output $|I| L_{\text{load}}$, shown as a dashed line, which is obtained from the measured current increase ΔI per rotation. This is equivalent to $\text{emf} \times I \times \Delta t$, but, in order that eddy current effects can be completely neglected, the experiments are done at a very low speed which is not necessarily constant. This prohibits good emf measurements. The zero current line represents pure loss since there is no output.

There is a marked maximum of the losses between 1 and $2 \times 10^{-4} \text{ V}\cdot\text{sec}$, followed by a minimum and a gradual increase towards higher values of P. The average field in front of the poles is also given in Fig. 8 and by comparison it is seen that the maximum occurs between 1 and 3 kG, i.e., below the upper critical field. This means that there is no properly normal zone developed at the center of the pumping spot; the entire spot pins the flux, hence the big loss. Above 3 kG there is a normal zone, the

pinning area is only at the edges of the spot and the losses are smaller. Another way of saying the same thing is: below H_{c2} the resistance in the spot has to be created entirely by exceeding the critical current locally which is done by induction from the moving pole pieces, i.e., by the distortion of the flux pattern.

The input increases with the load current but now there is an output which according to Eq. (3) is proportional to IP (given as thin line in Fig. 8a) minus $L_p I^2$, with L_p being the effective inductance of the current path around the spot. From both the 1600 A and 3200 A results one obtains $L_p = (3.75 \pm 0.02) \times 10^{-8}$ H. We further notice the current limit for low P values, when $P = L_p I$ and the emf becomes zero. The current limit for high values of P can have various origins as seen later. This pump reached a maximum current of 5000 A at about 0.2 mV·sec for P .

The results for the power efficiency, which is the ratio of output to input, is given in Fig. 8b. One is usually interested in the total energy efficiency (total energy input/total energy stored in the circuit), and with the efficiency being zero for zero current, this value is considerably lower. In the best case, it is between 20 and 30% for this pump.

By subtracting the output from the input one obtains the losses. In discussing these we try using Eq. (4) and obtain first the effective $I(0)$ for the zero current losses which has values between 4500 A for the maximum loss and 3100 A for the minimum. Adding to these values the actual transport current, 1600 A or 3200 A respectively, and using again Eq. (4) gives calculated values which are higher than the measured ones. The differences are plotted in Fig. 8c. The result is not surprising and indicates that the current density around the spot represents now part of the load current, while under zero current conditions it was purely induced without being much different as such. It is also interesting to note that the relaxation angle, given in Fig. 8e together with an outline of the rotor, has its maximum where the measured loss is largest relative to the calculated loss (maximum in the loss difference curves Fig. 8c). If one presumes that with the rotor relaxed, the transport current is more or less uniformly distributed, then the movement over the relaxation angle produces the nonuniformity discussed earlier and with it the enlarged extended critical regions.

Here another observation may be made relating to the torque. After unwinding through the full relaxation angle, the rotor will either come to rest at zero torque and will need a smaller torque in the opposite direction to drive the pump backwards, or, if the current is high enough, the rotor will continue unwinding with a small steady torque remaining until at a lower current this torque becomes zero. If, in this latter case, the unwinding torque is made zero, ω will be limited by eddy current losses. This spontaneous unwinding, or operation of the pump as a motor, is observed for $0.2 < P < 0.5$ mV·sec and for currents above 900 A.

Another way of discussing the losses would be to take the zero current loss as a pinning loss in addition to any current switching losses calculated as $L_p I^2$. After subtracting both the zero current loss and the switching loss there is still a fairly large loss left which would be interpreted as coming from increased critical regions (see Fig. 8d). The large relaxation angles would correspond to this increase in critical regions.

Neither of the two ways of looking at the losses is very satisfactory and this illustrates very well the shortcomings of the simple theory using only two parameters L_p and $I(0)$. This is, perhaps, even better seen when one tries to locate the regions where the losses actually occur. Such information can be extracted from field plots as given in Fig. 5. Figure 9 gives a complete field plot constructed from radial and tangential components and further indicates the places where the flux density changes in fields below 3 kG and, consequently, where there are losses. These are the places where the critical current is exceeded or, equivalently, where the flux moves against pinning forces.

This discussion suggests the principles for designing pumps of higher efficiency. To reduce the losses one has to reduce the area of critical regions surrounding a spot, and to increase the output one has to increase P . A rotor with a minimum number of large poles (usually two) and a good flux return path are suggested.

Such pumps have been built. Lubell will mention an example with a measured total energy efficiency of 60%.¹⁵

There is no reason why, with some development effort directed towards improving the rotating field pattern by shaping the rotor poles and the flux return path, an optimal efficiency could not be reached which is close to its theoretical limit. The term optimal is used to indicate that the efficiency would probably depend on current level, power output, and sense of rotation. The question is only whether the increased complexity and sophistication are a fair exchange for a saving in liquid helium, and the answer may depend on economic decisions.

Ultimate Current

The pumps of higher efficiency generally use iron as a good flux return path mainly to increase P . This also increases L_p in Eq. (3) and therefore reduces the maximum current reached: $I_{\max} = P/L_p$. The pump mentioned in the last paragraph has a current limit of about 2500 A. Van Houwelingen and Volger¹⁰ used six similarly designed pumps in parallel to produce a record of 12 800 A. The problem we want to discuss is how do we design a single pump to give a large current?

The pump used for the experiments described below is illustrated in Fig. 10. It has a corrugated sheet of 0.001 in. thick Nb foil. The corrugations which provide a large contact area with liquid helium are about 1.5 mm deep and number an average of 20 per centimeter.

At first we focus on the effective L_p . From Eq. (4) it can be seen that L_p is associated with the energy lost in switching the transport current from the front of the spot to the back, but, from Eq. (3), it can be interpreted as describing the flux due to the transport current and linked with the spot in opposition to the active pumping flux P . If this flux, $L_p I$, becomes equal to P , the pumping stops because the net flux linked with the moving spot is zero. That this second view is more adequate for the present problem is demonstrated in a comparison of the measured effective L_p with the calculated L_p of the path with the smallest inductance around the spot. Such values are found in Fig. 11 which also illustrates the dependence of L_p on the geometry of the rotor. The scale of the rotors and pole faces is indicated in the figure, the thickness of the poles being 1.2 cm. The smallest inductance is calculated for a loop of wire about 2 mm thick (roughly the thickness of the corrugated sheet) which surrounds the pole face area. Taking a thinner wire would increase the inductance because of the higher field at the surface of the wire and taking a thicker wire increases it also because the loop becomes bigger if the central hole stays the same. For similar reasons a wider portion of the sheet surrounding the spot also has a larger inductance.¹⁶ It is seen that the measured effective L_p values are an order of magnitude smaller than the calculated minimum inductances while the ratios between the three are comparable in both groups and also similar to the ratios of the pole face areas (0.44, 0.64; 1.24 cm² for the 8, 4, and 3 pole rotor).

15. M.S. Lubell and S.L. Wipf, in Advances in Cryogenic Engineering (Plenum Press, 1968), Vol. 13, p. 150.

16. F.W. Grover, Inductance Calculations (Van Nostrand, 1946; Dover, 1962).

These results imply good pump performances up to limiting currents of the order of 10^5 A, taking P of the order of 10^{-4} V.sec, if the pumping sheet and the circuit are capable of carrying such currents. If Nb is taken as a pump sheet then generally a current density of approximately 8×10^4 A/cm² can be expected in a field of 1 kG perpendicular to the sheet, and about half this value if the field is 2 kG. Above 3 kG the performance drops rapidly. This experience agrees very well with the average published current densities of cold-worked Nb.¹⁷ Circuits from commercial high field superconductors, stabilized by copper, can easily be dimensioned to take any required current. Connections to the sheet are made by spot welding between the superconducting materials, and superconducting joint currents in excess of 100 A per spotweld are quite common.

Using the three rotors of Fig. 11 (and other rotors) in the pump of Fig. 10, whose sheet and circuit are capable of currents exceeding 20 000 A, a new performance limiting phenomenon is experienced as was already observed as shown in Fig. 5 and has been described as an instability. It is a sudden breakdown and rearrangement of the current distribution in the sheet and usually happens at a current density which would correspond to a surface power density of 2 W/cm² if the sheet were normal. It is tempting to associate this current density level with the criterion for what has been described as enthalpy stabilization¹⁸; the evidence so far is too tenuous to construct a definite connection. For the corrugated Nb sheet used here and described above, this current level is at about 6000 A. In Fig. 12 are seen examples of current and voltage traces vs time for each of the three rotors at a constant low rotation speed (the 8-pole trace and the beginning of the 3-pole trace include a number of rotations in the opposite direction at the same speed). The instabilities are seen as voltage spikes but these spikes can have either direction, positive in the 8-pole case, negative in the 3-pole case. The net effect of the instability caused current redistribution in terms of shift of flux is not at all obvious; it may reduce the pumping process as in the 3-pole case or, seemingly, aid it.

The size and the direction of the current redistribution depend considerably on the shape of the rotor and, if the direction is different for the 3- and 8-pole rotors, there should be a case in between for which it is zero. The 4-pole rotor has indeed a much smaller instability activity but the over-all current limit is still given by an instability somewhere above 10 000 A. In this kind of process the current then falls back to around 5000 A. This current limit may be more characteristic of the sheet itself rather than the number and shape of the poles since at this current density all criteria for current stability in superconductors are greatly exceeded. The question of instabilities is complicated by the dependence on speed of rotation. Increasing the speed results in stronger and more frequent (per number of rotations) instabilities and also in a lowering of the final, instability governed, current limit. This dynamic dependence of flux jumping is generally connected¹⁹ with the viscous motion of flux, also named flux creep,²⁰ which is equivalent to a finite resistance of the superconduc-

-
17. C.S. Tedmon, R.M. Rose, and J. Wulff, in Metallurgy of Advanced Electronic Materials (Interscience, Philadelphia, 1962), Vol. 19, p. 89;
D. Kramer and C.G. Rhodes, Trans. Met. Soc. AIME 233, 192 (1965);
W. DeSorbo, Phys. Rev. 134, A1119 (1964);
M.A.R. LeBlanc and W.A. Little, in Proc. 9th Intern. Conf. Low Temperature Physics, Toronto, 1960, p. 362.
 18. R. Carruthers, D.N. Cornish, and R. Hancox, in Proc. 1st Intern. Cryogenic Conference, Kyoto, 1967 (Heywood Temple), p. 107.
 19. S.L. Wipf, Phys. Rev. 161, 404 (1967).
 20. Y.B. Kim, C.F. Hempstead, and A.R. Strnad, Phys. Rev. 131, 2486 (1963).

ting material. For a closed superconducting circuit flux creep is experienced as a slow decay of the current. It has been suggested²¹ that such a decay be logarithmic in time.

However, the decay observed in the present case is different from any simple model. Figure 13 shows current traces vs time on a greatly enlarged current scale (see bar representing 10 A). They are obtained by pumping at various constant rates to the current stated and then stopping the rotation of the pump. The decay, always fairly rapid immediately at the beginning, is practically finished after about 20 min and the total current reduction is of the order of 10 A. The decay curves for a higher current never reach the ones for a lower current nor are the lower ones similar in shape to a portion of the higher ones after a certain time interval. This is borne out by the example of the 10 000 A case where, after a decay of 50 min and 25 A, the original current level is regained by three full rotations (which included several instabilities, one of which reduced the current by about 15 A as shown in the tracing in Fig. 13) and the ensuing decay curve is quite different. Also a very long decay run made at 11 000 A showed no decay bigger than $\sim 1\%$ (equivalent to the drift of the recording equipment) over 40 hours. These decays have to be attributed to a relaxation of the current distribution in the sheet which, as we concluded earlier, has after all a resistive region (current induced) when the spots are moving. At the end of the decay the current distribution must have reached an equilibrium distribution in a then fully superconducting sheet.

These observations will also have importance when pumps are used to measure very high critical currents; in general, it will be necessary to make the load inductance sufficiently large.

IV. CONCLUSION

We have shown the inadequacy of the mathematical treatment which does not account for the existence of critical regions in the sheet of a moving magnetic field flux pump. The losses in the critical regions are of the same nature as the ac losses discussed earlier and they contribute heavily to the over-all losses in the pump. The instability of the critical regions limits the ultimate output current. A good pump design is one which minimizes the extent of critical regions and avoids instabilities. To fulfill both conditions in the same pump design may not be possible. The analytical difficulties leave many design problems to intuitive solutions. This is characteristic of the present-day art of flux pump making, and scientists, of course, are always a little suspicious of artists.

21. Y.B. Kim, C.F. Hempstead, and A.R. Strnad, Phys. Rev. Letters 9, 306 (1962);
P.W. Anderson and Y.B. Kim, Rev. Mod. Phys. 36, 39 (1964);
J. File and R.G. Mills, Phys. Rev. Letters 10, 93 (1963);
J. File, J. Appl. Phys. 39, 2335 (1968).

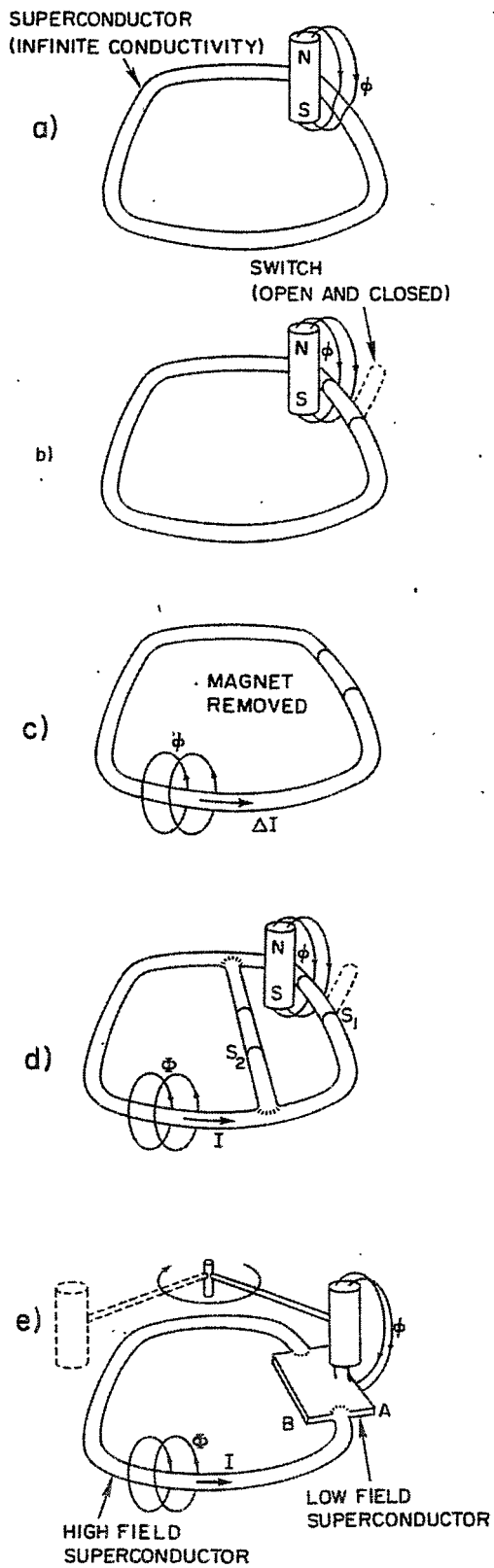


Fig. 1. Principle of flux pumping.

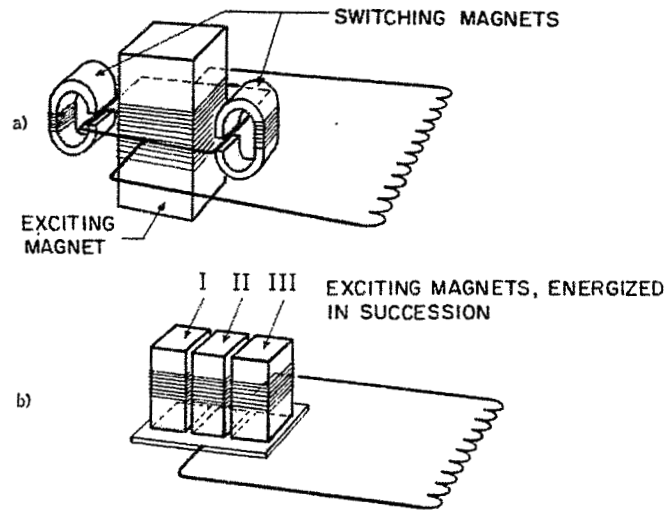


Fig. 2. Two arrangements of flux pumps without moving parts (from Ref. 9). The upper example is a rectifier type [see Ref. 5 and J.L. Olsen, *J. Appl. Phys.* **29**, 537 (1958); R. Fasel and J.L. Olsen, in Proc. 11th Intern. Congress on Refrigeration, Madrid, 1967; also in *Z. Kältetech. Klimat.* **19**, 274 (1967)]. The lower example uses a moving magnetic field. This version is feasible but ineffective because of the poor shape of the normal spot (large critical regions, high L_p) [see S.L. Wipf, in Advances in Cryogenic Engineering (Plenum Press, 1964), Vol. 9, p. 342; D. Van Houwelingen et al., *Phys. Letters* **8**, 310 (1964); B.S. Blaisse et al., *Phys. Letters* **14**, 5 (1965)].

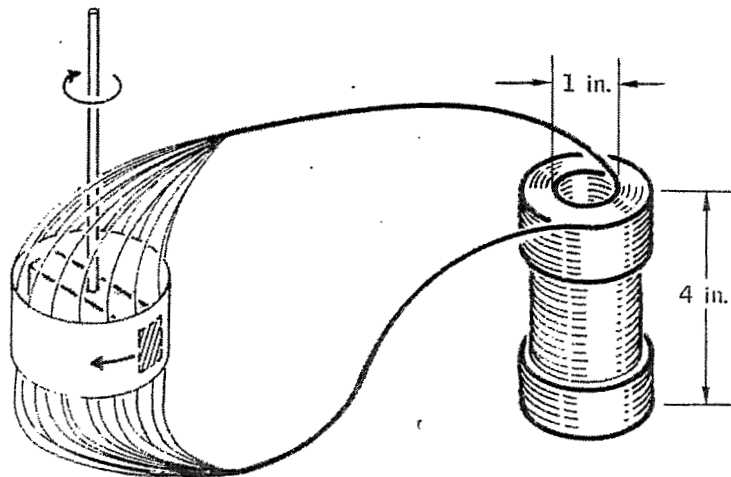


Fig. 3. Typical example of moving magnetic field flux pump. Not shown here are coils to magnetize the iron rotor so that the poles all have the same magnetic polarity, see Fig. 6 (from Ref. 15).

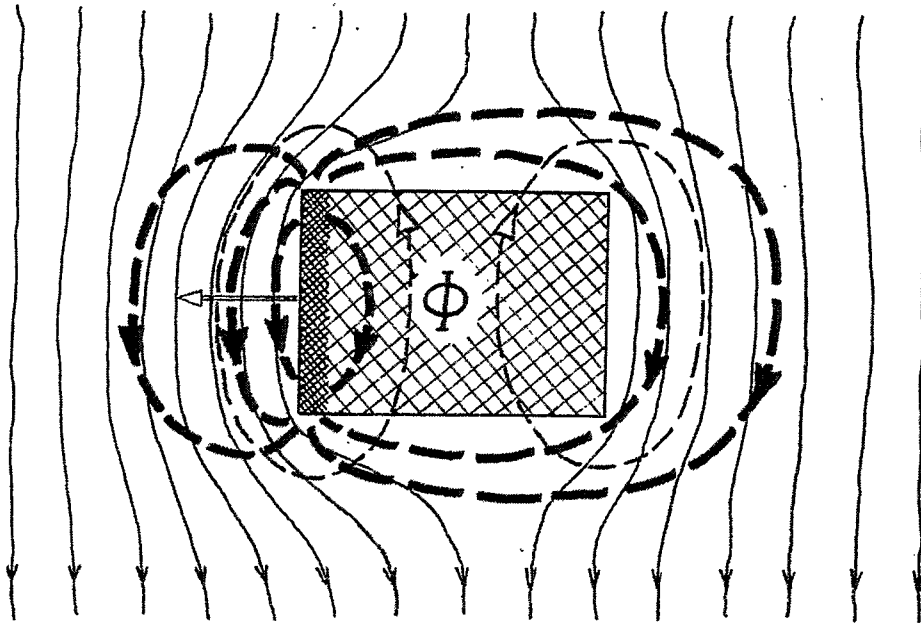


Fig. 4. Schematic current distribution around moving normal spot containing flux Φ :

- Horizontal arrow : Direction of movement
- Crosshatch : Resistive (normal) region
- Narrow crosshatch : Leading edge
- Thin solid lines : Load current distribution
- Thin broken lines : Eddy current distribution
- Thick broken lines : Alternative current distribution for current which is driven resistively out of the leading edge.

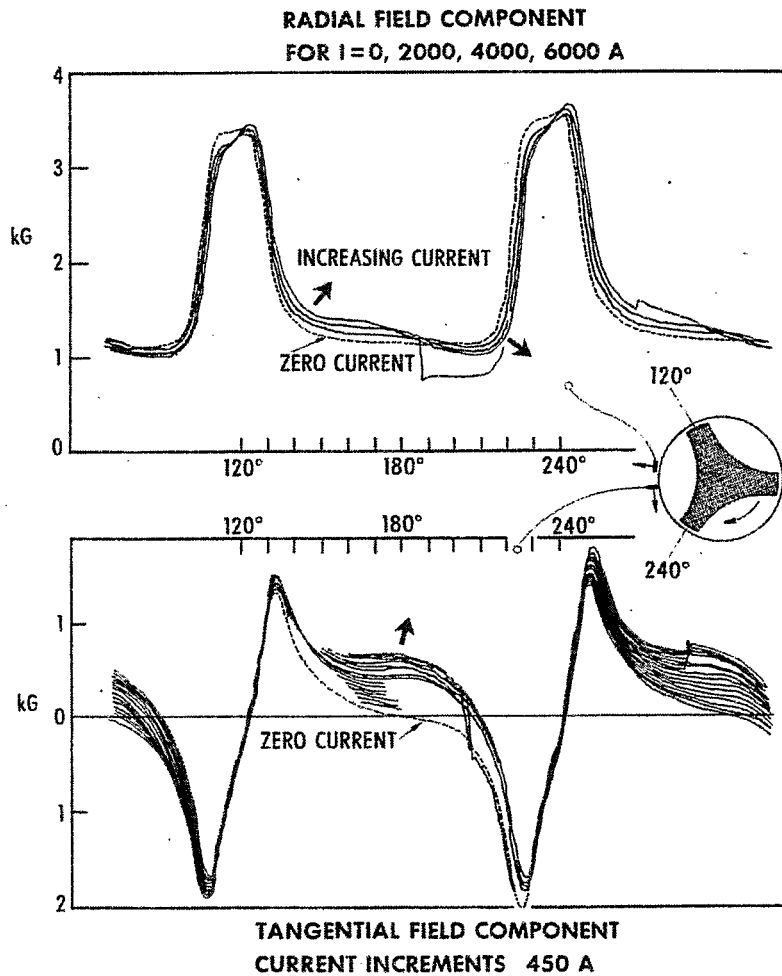


Fig. 5. Radial and tangential field components vs angle (relative to rotor). Measured by stationary Hall probes at the outer surface of the pumping sheet and at the center of the path of the pumping spot. The diameter of the sheet is 7.9 cm, the rotor diameter 7.6 cm, width of pole face 1.35 cm, thickness of rotor 1.22 cm. The distance of the center of the Hall probe from the surface of the sheet is 0.3 cm. (The pump is shown in Fig. 10 with a different sheet.)

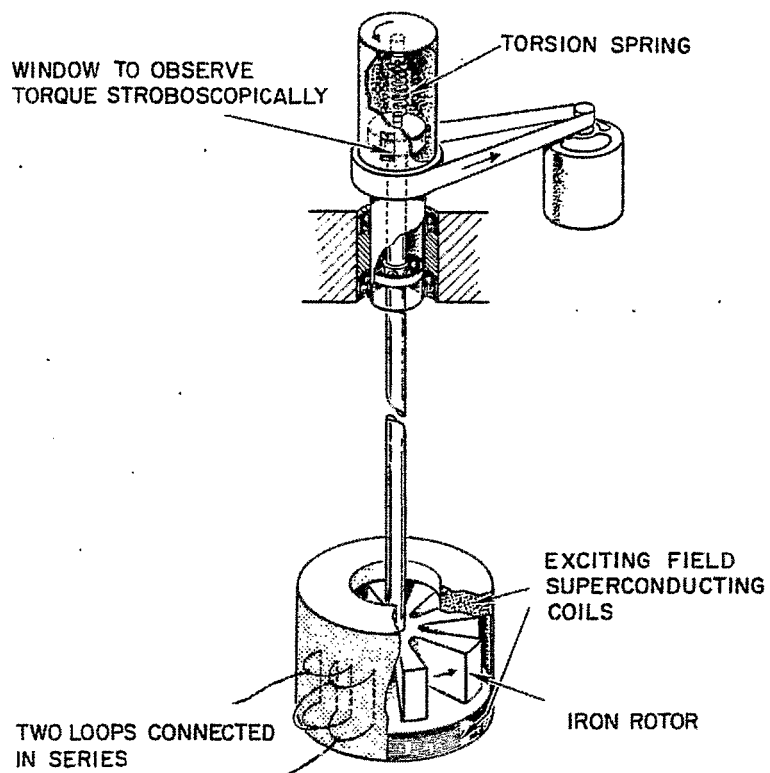


Fig. 6. Example of pump used to measure losses (from Ref. 9). The exciting coils are energized in series opposition to give all poles the same polarity.

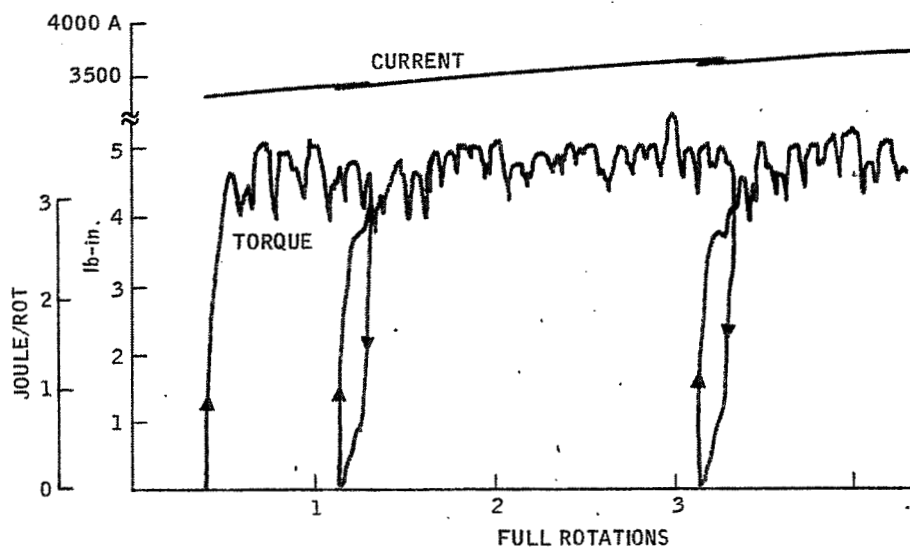
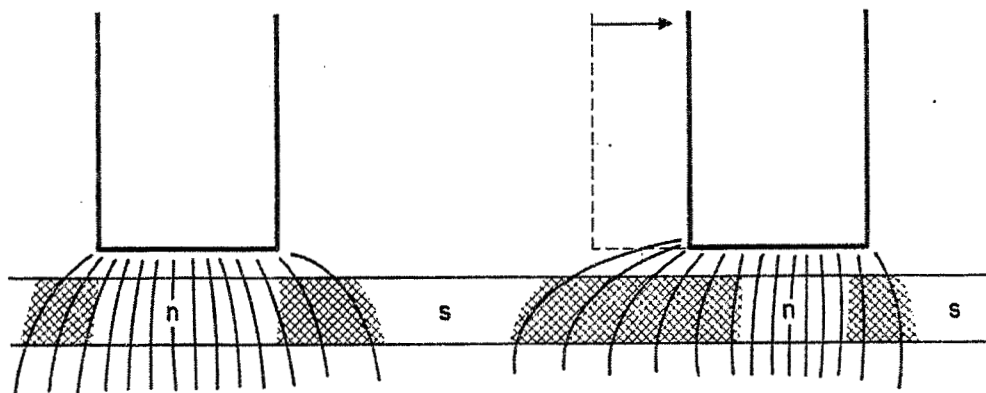


Fig. 7. XY traces of input torque and output current vs rotation angle for pump with a sheet of 7.0 cm diameter and a rotor illustrated in Fig. 8e. Above: illustration of relaxation angle in terms of flux pinning (see text).

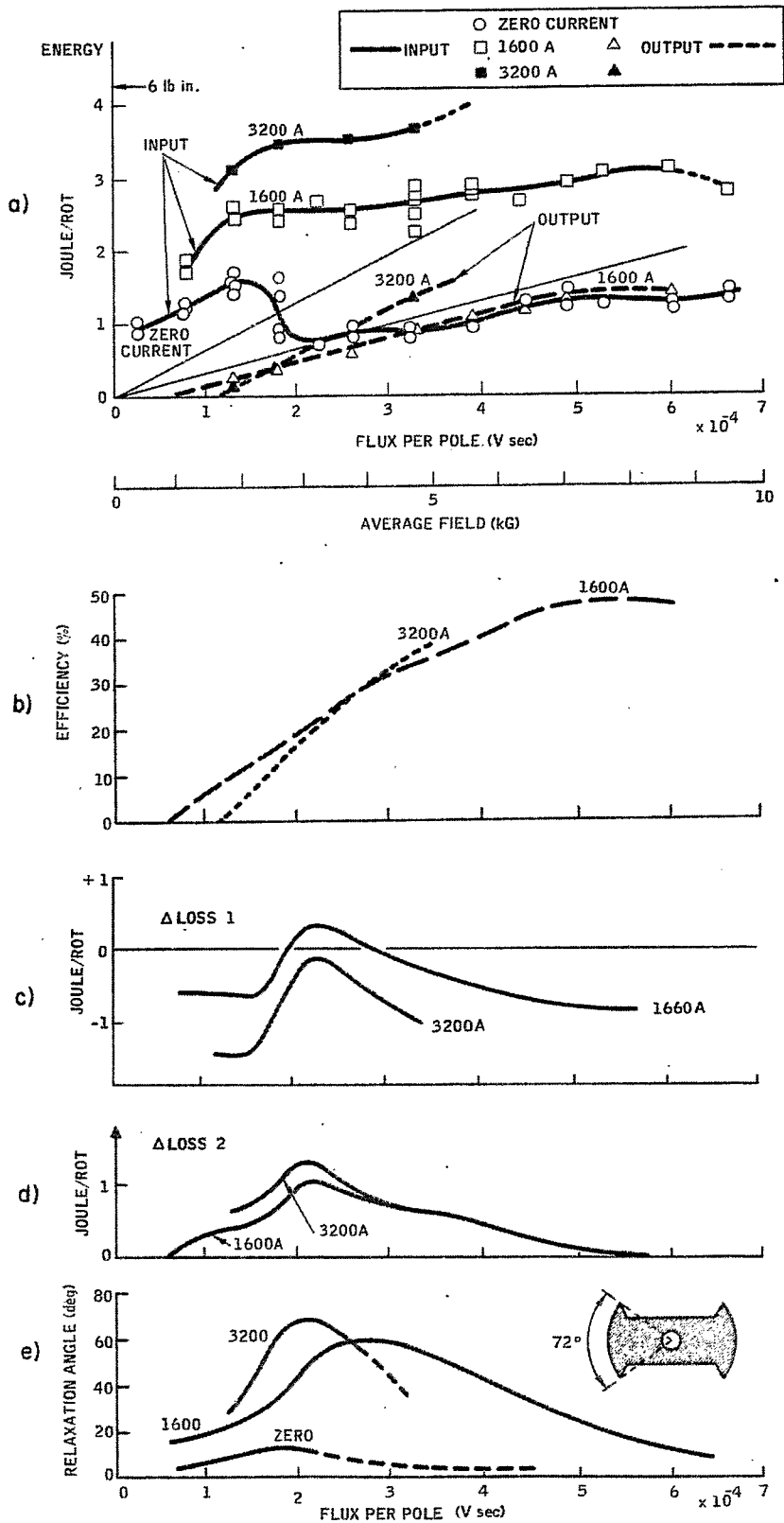


Fig. 8. a) Input and output power vs flux per pole (P) and vs average field in front of poles. For 0, 1600, 3200 A output current.
 b) Power efficiency (output/input power) vs P.
 c) and d) Difference between Eq. (4) and measured losses with two different interpretations of I(0) (see text).
 e) Relaxation angle vs P. Insert: outline of rotor, diameter 6.72 cm, thickness 1.78 cm.

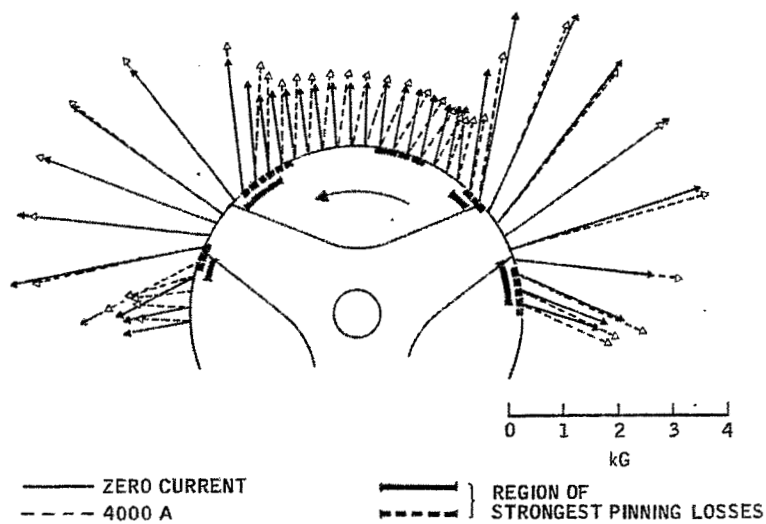


Fig. 9. Field distribution constructed from Fig. 5 for zero and 4000 A currents, with indication of extent of critical regions.

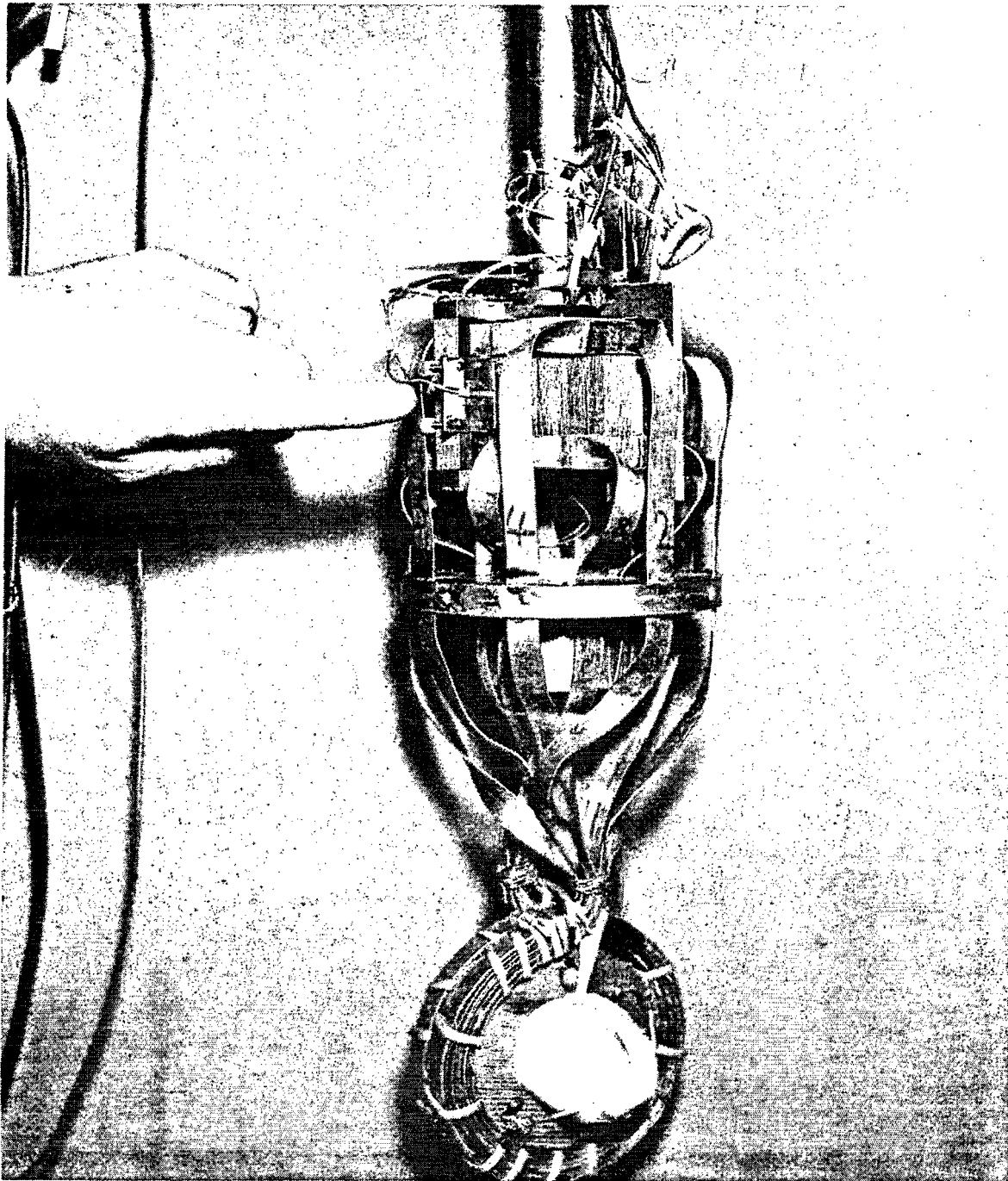
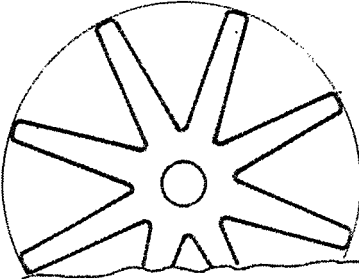
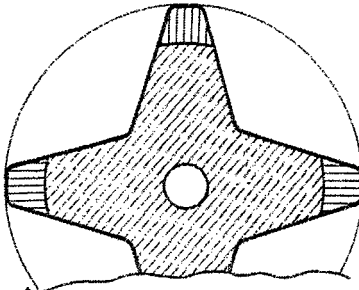
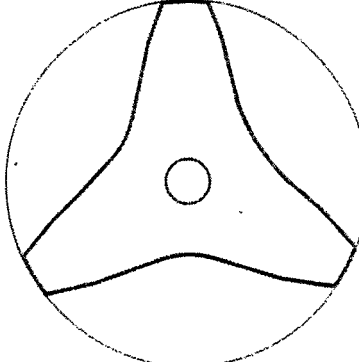


Fig. 10. Example of flux pump for high currents. Circuit consists of 8 tapes of NbTi strip sandwiched between copper strips. The current produces 0.230 G/A at the center of two turns of 9.0 cm i.d. where it is measured by calibrated Hall probes. The finger points to Hall probes which are used to measure field profiles as in Fig. 5.

$$\text{emf} = n\omega (P - L_p I)$$

ONE POLE / TOTAL CURRENT

ROTOR	POLE FACE	L_p MEASURED (H)	L (LOOP) CALCULATED (H)
		4.5×10^{-10}	(5.7×10^{-9})
		1.15×10^{-9}	(8.1×10^{-9})
		1.93×10^{-9}	(1.42×10^{-8})

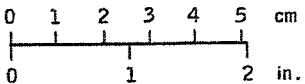


Fig. 11. Three different rotors used in pump of Fig. 10. Comparison of measured L_p with minimum inductance of loop around pole face. Rotors and pole faces are drawn to scale.

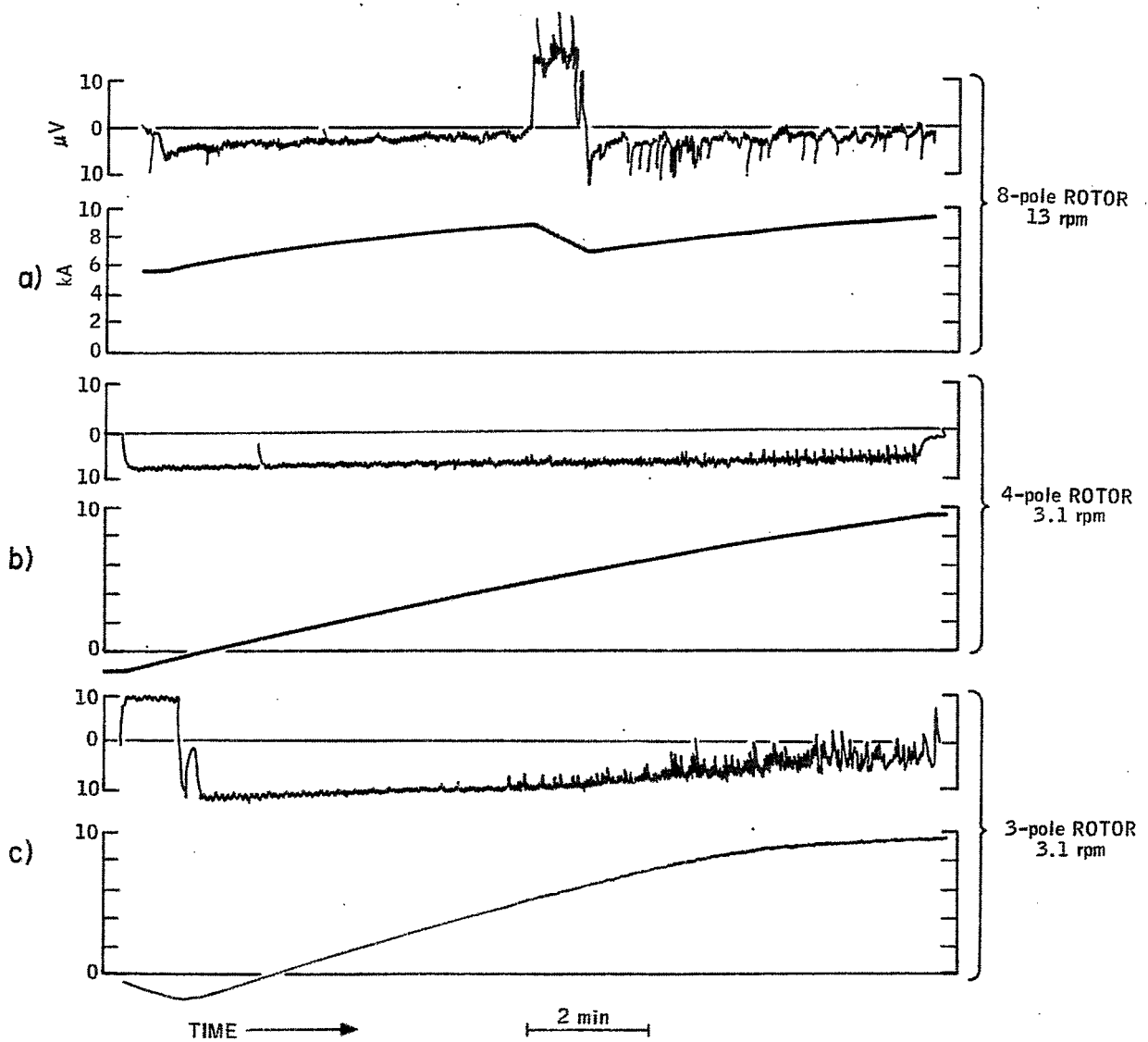


Fig. 12. Traces of emf (in μV) and output current (in kA) vs time for the three different rotors of Fig. 11 used in the pump of Fig. 10.

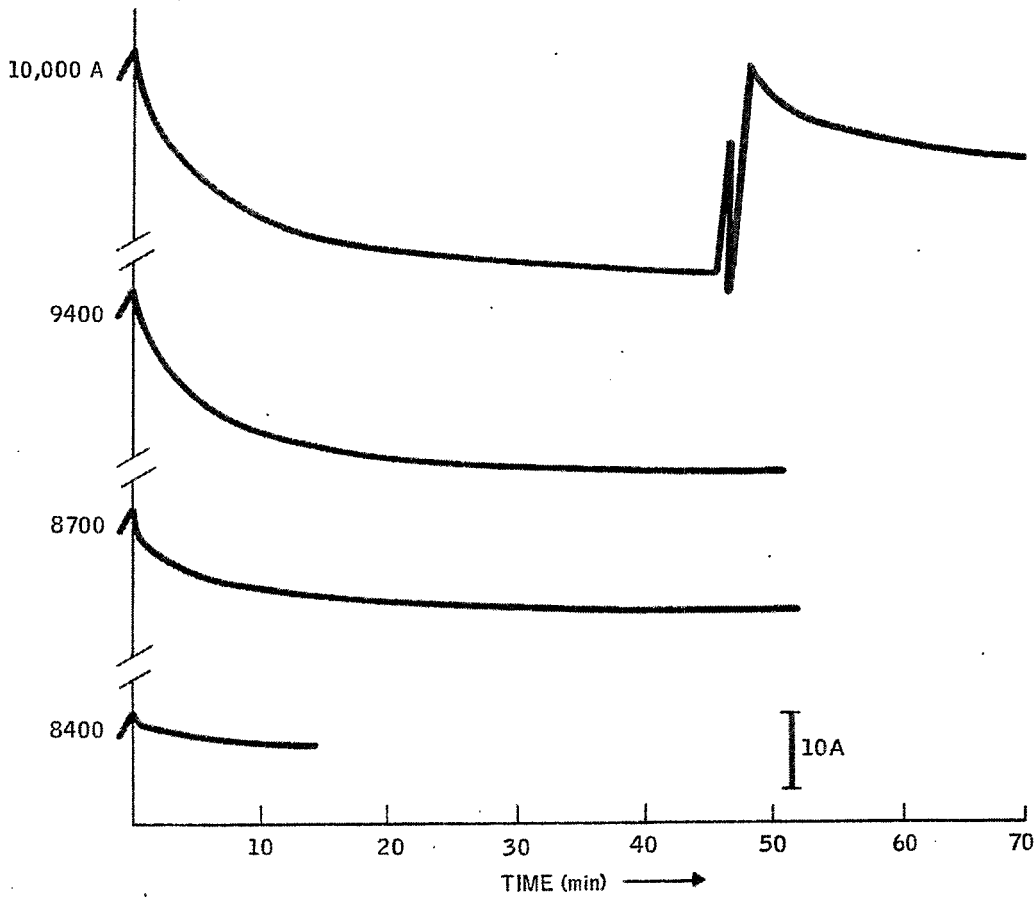


Fig. 13. Decay of current on expanded current scale (see scale for 10 A) vs time after pump has been stopped. Initial current indicated in amperes, 8-pole rotor, 10 rpm before stopping. Pump and rotor as in Figs. 10, 11.